J. Fluid Mech. (1976), *vol.* 74, *part* 2, *pp.* 375–399
Printed in Great Britain

Nonlinear energy transfer and the energy balance of the internal wave field in the deep ocean†

By DIRK J. OLBERS
Institut für Geophysik, Universität Hamburg, Germany

(Received 15 July 1975)

The source function describing the energy transfer between the components of the internal wave spectrum due to nonlinear interactions is derived from the Lagrangian of the fluid motion and evaluated numerically for the spectral models of Garrett & Munk (1972*a*, 1975). The characteristic time scales of the transfer are found to be typically of the order of some days, so that nonlinear interactions will play an important role in the energy balance of the wave field. Thus implications of the nonlinear transfer within the spectrum for generation and dissipation processes are considered.

1. Introduction

Our knowledge of internal wave motions in the interior of the ocean has advanced considerably in recent years as a combined result of improving instruments and ocean techniques and interpreting the data within the framework of linear internal wave theory. The progress in the last four years has been reviewed by Briscoe (1975), and Wunsch (1975) gave a critical survey of the observational techniques and data interpretation. Garrett & Munk (1972) made the first attempt to provide a unified picture of the wave field by reconstructing the complete wavenumber spectrum of the motion from the available data. Since then the model spectrum of Garrett & Munk (henceforth GM) has been slowly changing, partly because the parameters of the model have been measured more precisely, partly because the model has been extended at small scales to include the observed fine-structure under the hypothesis that this is due to internal waves (Garrett & Munk 1975).

Comparatively little is still known, however, about the dynamical processes which govern the internal wave field in the ocean and determine the energy level and the spectral shape. There are a large number of experimental and theoretical studies treating the generation and dissipation of internal waves (see the review by Thorpe 1975). Most of these studies consider the interaction of discrete waves with external fields and may not be applied to the balance of a spectrum. But even if the spectral input or dissipation rates of interaction processes are derived (cf. Müller & Olbers 1975) the evaluation might still be impossible because the space–time structure of the interacting fields is not sufficiently well known. This applies especially to the space–time spectra of atmospheric fluctuations. Some

† Contribution from the Sonderforschungsbereich 94 'Meeresforschung Hamburg'.

processes, such as wave breaking, for example, even resist altogether a rigorous theoretical treatment because a reasonable parametrization of their strongly nonlinear dynamics is lacking.

Nonlinear interactions within the internal wave field can be investigated without being restricted by these two principal difficulties: lack of the space–time structure or lack of a theoretical concept. A model of the wave spectrum exists, and the theory of nonlinear interactions among waves is well known and has been applied with success to many geophysical fields, including internal waves. Weak resonant interaction among discrete internal waves has been studied by Ball (1964) and Thorpe (1966). Hasselmann (1966, 1967) has extended the theory to a continuous spectrum of resonantly interacting wave components. Kenyon (1968) has evaluated the energy transfer rates in an ocean with linear stratification for a low mode spectrum which is unfortunately in strong contrast to the GM model. Parallel to these theoretical investigations laboratory experiments have been carried out to demonstrate resonant interactions for progressive (Martin, Simmons & Wunsch 1969, 1972) and standing internal waves (McEwan 1971; McEwan, Mander & Smith 1972). Neshyba & Sobey (1975) even attempted to trace resonant triplets of internal waves in the ocean by means of bispectral analysis of temperature records from vertically separated sensors.

In this paper we derive the source function for resonant interaction of internal waves in a WKBJ representation starting with a Lagrangian description of a rotating Boussinesq fluid to include the effect of the Coriolis forces. The source function is evaluated numerically for the GM model and the resulting energy transfer within the spectrum and the characteristic time scales are discussed. It is found that nonlinear interactions transfer energy from medium frequencies and wavenumbers to high wavenumbers at low and high frequencies, with a transfer rate which increases with the square of the local Brunt–Väisälä frequency. With a characteristic transfer time of some days in the main thermocline, wave–wave interaction can be expected to play an important role in the energy balance of the internal wave field.

Thus, as in the surface wave problem (Hasselmann *et al.* 1973), the nonlinear energy transfer within the spectrum may serve as a frame which other processes should fill if they contribute significantly to the energy balance. The nonlinear transfer rate then implies restrictions on the effectiveness of these processes. This is discussed for the generation and dissipation of inertial waves, and dissipation of internal waves by wave breaking.

2. Lagrangian description of a Boussinesq fluid

Linear wave trains and weak nonlinear interactions among them are suitably treated with a Lagrangian description of the fluid motion. If a variational principle is available which produces the equations of motion the lengthy and cumbersome derivation of the WKBJ approximation of a vector problem to first order can be avoided by the method of the averaged Lagrangian (see Whitham 1965, 1970; Dewar 1970; Dougherty 1970; Bretherton 1971; Olbers & Richter 1973). Treating wave–wave interactions within a Lagrangian framework

has the advantage of dealing with a scalar perturbation analysis and, moreover, yields symmetrical coupling coefficients (Hasselmann 1966, 1967).

The Lagrangian equations of motion of a fluid in a rotating co-ordinate system are given by† $$\rho\{\ddot{x}_j + \epsilon_{jkl} f_k \dot{x}_l + \delta_{j3} g\} = -\partial p/\partial x_j. \tag{2.1}$$

Here ρ and p are the (Eulerian) density and pressure field at the instantaneous position $x_j(\mathbf{r}, t)$ of a fluid parcel which in an initial state was at the position r_j with the initial density $$\rho_L(\mathbf{r}) = \rho(\mathbf{x}, t)\, \partial(x_1, x_2, x_3)/\partial(r_1, r_2, r_3). \tag{2.2}$$

If the fluid is incompressible the volume of each fluid parcel does not change on its path. Thus $$\partial(x_1, x_2, x_3)/\partial(r_1, r_2, r_3) = 1 \tag{2.3}$$

and $\rho_L(\mathbf{r}) = \rho(\mathbf{x}, t)$.

Equation (2.1) and the constraint (2.3) may be derived from Hamilton's principle $$\delta \int dt\, d^3r\, \mathscr{L}(x_j, \dot{x}_j, \partial x_j/\partial r_k, \mathbf{r}, t) = 0 \tag{2.4}$$

using the Lagrangian density

$$\mathscr{L} = \tfrac{1}{2}\rho_L\{\dot{x}_j \dot{x}_j + \epsilon_{jkl} f_j x_k \dot{x}_l\} - \rho_L g x_3 + \lambda\{\partial(x_1, x_2, x_3)/\partial(r_1, r_2, r_3) - 1\} \tag{2.5}$$

with the Lagrangian multiplier $\lambda(\mathbf{r}, t) = p(\mathbf{x}, t)$.

The Boussinesq approximation is obtained by expanding the fields x_j and λ about a state of hydrostatic equilibrium $\dot{x}_j = 0$ and neglecting variations in density in so far as they affect inertia but retaining them in the buoyancy terms. We define the deviations from equilibrium by

$$\xi_j(\mathbf{r}, t) = x_j(\mathbf{r}, t) - r_j, \quad \pi(\mathbf{r}, t) = \lambda(\mathbf{r}, t) - \overline{p}(x_3). \tag{2.6}$$

The equilibrium pressure $\overline{p}$ is related to the mean density field $\overline{\rho}$ by

$$d\overline{p}/dr_3 = -g\overline{\rho}(r_3). \tag{2.7}$$

The Lagrangian of the Boussinesq approximation then becomes

$$\mathscr{L}_B = \tfrac{1}{2}\rho_0\{\dot{\xi}_j \dot{\xi}_j + \epsilon_{jkl} f_j \xi_k \dot{\xi}_l\} + \pi\{\partial \xi_j/\partial r_j + \Delta_{jj} + \Delta\} - \Phi(\xi_3), \tag{2.8}$$

where ρ_0 is a constant average density and Δ_{jk} is the cofactor of $\partial \xi_j/\partial r_k$ in

$$\Delta = \det(\partial \xi_j/\partial r_k) = \Delta_{jk}\, \partial \xi_j/\partial r_k. \tag{2.9}$$

The equilibrium state appears only in the external potential

$$\Phi(\xi_3) = g\overline{\rho}(r_3)\, \xi_3 + \overline{p}(r_3 + \xi_3), \tag{2.10}$$

which is the potential of the buoyancy field. Expansion yields

$$\Phi(\xi_3) = \overline{p}(r_3) + \tfrac{1}{2}\rho_0 N^2(r_3)\, \xi_3^2 + \sum_{n=3}^{\infty} \frac{1}{n!} \xi_3^n \frac{d^n \overline{p}}{dr_3^n}, \tag{2.11}$$

where $$N^2(r_3) = \frac{1}{\rho_0}\frac{d^2\overline{p}}{dr_3^2} = -\frac{g}{\rho_0}\frac{d\overline{\rho}}{dr_3} \tag{2.12}$$

is the squared Brunt–Väisälä or buoyancy frequency.

† We use a right-handed co-ordinate system (r_1, r_2, r_3) with the r_3 axis pointing upwards. The Coriolis vector (f_1, f_2, f_3) will be vertical in the later sections $(f_3 = f)$. $\epsilon_{jkl} = 1(-1)$ if (jkl) is an even (odd) permutation; $\epsilon_{jkl} = 0$ otherwise.

We notice two nonlinear forces which act on the fluid motion. The first arises from the incompressibility constraint; the second is due to non-quadratic terms in the buoyancy potential. The ratio of these two forces can be estimated as

$$\pi\Delta_{jj}/\xi_3^3\frac{d^3\overline{p}}{dr_3^3} = O(k_3 L_v), \tag{2.13}$$

where k_3 is a mean vertical wavenumber of the motion and L_v is the vertical scale of the Brunt–Väisälä frequency. The ratio of the inertial to the nonlinear forces follows from

$$\rho_0\xi_3^2/\pi\Delta_{jj} = O(1/k_3\xi_3) \tag{2.14}$$

while the terms which have been omitted as a consequence of the Boussinesq approximation are related to the remaining inertial terms by

$$\rho_0\xi_j^2/\delta\rho\,\xi_j^2 = \rho_0/\delta\rho \approx 10^3, \tag{2.15}$$

with $\delta\rho = \overline{\rho} - \rho_0$. For internal wave motion representative values are $\xi_3 = 10\,\mathrm{m}$, $k_3 = 2\pi/260\,\mathrm{m}$ and $L_v = 1300\,\mathrm{m}$ (average values taken from Garrett & Munk 1972*a*). Then

$$\rho_0\xi_3^2 \;:\; \pi\Delta_{jj} \;:\; \xi_3^3\frac{d^3\overline{p}}{dr_3^3} \;:\; \delta\rho\,\xi_3^2 \;\approx\; 10^3 \;:\; 2\times10^2 \;:\; 10 \;:\; 1,$$

which justifies successively the Boussinesq approximation, which has already been applied, a WKBJ approximation in the vertical by which nonlinear buoyancy forces are shifted to higher orders, and linearization, i.e. treating the nonlinear forces as a weak perturbation of the linear state.

3. Internal waves in the WKBJ approximation

The rich vertical structure of internal wave motion can be seen in vertical profiles of temperature (Cairns 1975) and current (Sanford 1975). Indirect evidence of the small vertical scale of the motion is given by the rapid drop of coherences of current and temperature data over increasing vertical separations of the sensors (Siedler 1971; Webster 1972). Also, the 'WKBJ normalization' of the observed spectra works extremely well (Fofonoff & Webster 1971; Briscoe 1975*b*; Hayes, Joyce & Millard 1975).

3.1. *Linear internal waves*

If the scales of the background are large compared with the wavelength, i.e. $k_3 L_v \gg 1$, the wave field can be represented as superposition of propagating wave trains. An internal wave train is of the form

$$\begin{Bmatrix}\xi_j\\ \pi\end{Bmatrix} = a\begin{Bmatrix}Z_j\\ P\end{Bmatrix} e^{i(\mathbf{k}.\mathbf{r}-\omega t)} + \text{c.c.}, \tag{3.1}$$

where the amplitude a, wave vector $\mathbf{k}$, frequency ω, and the relative amplitudes Z_j and P vary slowly compared with the rapid phase variations. This slow time and space dependence can be obtained by a WKBJ analysis or, more elegantly, by Whitham's method of the averaged Lagrangian (Whitham 1965, 1970; Dewar 1970; Dougherty 1970; Bretherton 1971).

We substitute (3.1) into the 'linearized' form of $\mathscr{L}_B$ and average over the phases. This yields Whitham's averaged Lagrangian†

$$\Lambda = |a^2|\{\omega^2 Z_j Z_j^* - N^2 Z_3 Z_3^* - i\omega f(Z_2 Z_1^* - Z_1 Z_2^*) + ik_j(Z_j P^* - P Z_j^*)\}. \quad (3.2)$$

Variation of Λ with respect to the relative amplitudes Z_j and P yields a system of linear equations which determine Z_j and P as

$$Z_j = C\begin{cases} ik_1 - (f/\omega)\,k_2 & (j=1), \\ ik_2 + (f/\omega)\,k_1 & (j=2), \\ -i\dfrac{\omega^2 - f^2}{N^2 - \omega^2}k_3 & (j=3), \end{cases} \quad (3.3)$$

and

$$P = C(\omega^2 - f^2) \quad (3.4)$$

up to a suitable real normalization constant C, provided that the frequency and the wave vector obey the dispersion relation

$$\omega = \Omega(\mathbf{k}, \mathbf{r}, t) \equiv \left[N^2\frac{\alpha^2}{k^2} + f^2\frac{\beta^2}{k^2}\right]^{\frac{1}{2}}. \quad (3.5)$$

Here k, α and β are the moduli of the total, horizontal and vertical wave vectors, respectively, and the square root is taken positive. From the existence of a dispersion relation one obtains the ray equations

$$\left.\begin{aligned} \dot{r}_j &= \partial\Omega/\partial k_j \equiv v_j, \quad \text{say}, \\ \dot{k}_j &= \partial\Omega/\partial r_j, \end{aligned}\right\} \quad (3.6)$$

which determine wave group trajectories in $\mathbf{r}, \mathbf{k}$ space. Finally, modulations of the amplitude caused by the propagation follow from the variation of Λ with respect to the phase of the wave group. This yields

$$\frac{\partial}{\partial t}\frac{\partial\Lambda}{\partial\omega} - \frac{\partial}{\partial r_j}\frac{\partial\Lambda}{\partial k_j} = 0. \quad (3.7)$$

Because $\Lambda \equiv 0$ for the solutions (3.3)–(3.5) we have

$$d\Lambda = \frac{\partial\Lambda}{\partial\omega}d\omega + \frac{\partial\Lambda}{\partial k_j}dk_j = 0, \quad (3.8)$$

so that (3.7) may be written as

$$\left\{\frac{\partial}{\partial t} + \frac{\partial}{\partial r_j}v_j\right\}\frac{\partial\Lambda}{\partial\omega} = 0, \quad (3.9)$$

which expresses the conservation of wave action if we define the wave action density by $\partial\Lambda/\partial\omega$. This quantity is related to the wave energy density E by

$$E = \omega\,\partial\Lambda/\partial\omega - \Lambda = \omega\,\partial\Lambda/\partial\omega = 2\gamma|a|^2, \quad (3.10)$$

with

$$\gamma = \tfrac{1}{2}\{Z_j Z_j^*\omega^2 + Z_3 Z_3^* N^2\} = \left|C\frac{\omega\alpha k}{\beta}\right|^2. \quad (3.11)$$

Thus the action density is equal to the energy density of the wave divided by its frequency. In the presence of a mean current a Doppler shift must be added to $\Omega(\mathbf{k}, \mathbf{r}, t)$. Then the frequency ω in (3.10) must be identified with the intrinsic

† We shall set ρ_0 equal to 1, thus measuring energy density and pressure in $\mathrm{cm^2\,s^{-2}}$.

frequency, i.e. the frequency relative to the mean flow (Bretherton & Garrett 1968; Olbers & Richter 1973), if E is to retain its physical meaning as the energy density relative to the mean flow.

3.2. *Wave–wave interactions*

In the linear theory the waves move independently of each other through the background medium. Changes in the wave field occur only because the wave parameters – frequency, wave vector and amplitude – are slowly modulated by the inhomogeneities of the background. Proceeding to higher orders in the wave amplitudes we find that there are additional changes in the state of the wave field because the waves exert nonlinear forces on each other and exchange energy and momentum by resonant coupling.

The resonant interaction of waves has been developed in a Lagrangian framework by Hasselmann (1966, 1967, 1968) and applied to various geophysical wave fields. We can follow closely his concept with one exception. A rotating system as characterized by the Coriolis term in (2.8) is not invariant under time reversal in the sense of classical dynamics (it would be invariant against reversing the rotation vector in addition to the reversal of time and momenta). Therefore normal amplitudes as used by Hasselmann do not exist and we have to modify his concept slightly.

Because of the relation (2.13), the lowest order of the WKBJ expansion of the Lagrangian (2.8) is given by

$$\mathscr{L}_0 = \tfrac{1}{2}\{\dot{\xi}_j \dot{\xi}_j + \epsilon_{jkl} f_j \xi_k \dot{\xi}_l - N^2 \xi_3 \xi_3\} + \pi \left\{\frac{\partial \xi_j}{\partial r_j} + \Delta_{jj} + \Delta\right\}, \tag{3.12}$$

which contains only the nonlinearities arising from the incompressibility constraint

$$\frac{\partial \xi_j}{\partial r_j} + \Delta_{jj} + \Delta = 0. \tag{3.13}$$

A linear wave group satisfies this constraint only to the first order in the wave amplitude. A representation of the wave field which is correct to all orders in the wave amplitude can be obtained by expanding the displacement $\boldsymbol{\xi}$ in a series

$$\begin{aligned}\boldsymbol{\xi} = &\sum_0 a_0 \mathbf{Z}_0 \exp i(\mathbf{k}_0 . \mathbf{r} - \omega_0 t) \\ &+ \sum_{1,2} a_1 a_2 \mathbf{Z}_{12} \exp\{i(\mathbf{k}_1 + \mathbf{k}_2) . \mathbf{r} - i(\omega_1 + \omega_2) t\} + \ldots\end{aligned} \tag{3.14}$$

and computing the higher-order coefficients in terms of the lower-order ones by means of (3.13). We have simplified the notation by introducing $\omega_j = s_j \Omega(\mathbf{k}_j)$ with $s_j = \pm$ and using j for $(s_j, \mathbf{k}_j)$. Thus a_0 stands for $a^{s_0}_{\mathbf{k}_0}$, and for each dummy index j there is summation over the two sign possibilities $\omega = \pm \Omega(\mathbf{k})$ as well as over all wave vectors $\mathbf{k}$ (generally a continuum). If we take in accordance with (3.3)

$$\mathbf{Z}_0 = (\mathbf{Z}_{\bar{0}})^* = C_0 \begin{Bmatrix} i(\mathbf{k}_0)_1 - \dfrac{f}{\omega_0}(\mathbf{k}_0)_2, \\ i(\mathbf{k}_0)_2 + \dfrac{f}{\omega_0}(\mathbf{k}_0)_1, \\ -i\dfrac{\omega_0^2 - f^2}{N^2 - \omega_0^2}(\mathbf{k}_0)_3, \end{Bmatrix} \tag{3.15}$$

where $\bar{j}$ denotes $(-s_j, -\mathbf{k}_j)$, reality of ξ is achieved (with $C_j^* = C_{\bar{j}}$) by

$$(a_j)^* = a_{\bar{j}}. \tag{3.16}$$

The second-order expansion coefficient may then be chosen as

$$\mathbf{Z}_{12} = (\mathbf{Z}_{\bar{1}\bar{2}})^* = \frac{i}{2}\frac{\mathbf{k}_1+\mathbf{k}_2}{(\mathbf{k}_1+\mathbf{k}_2)^2}(\mathbf{k}_1.\mathbf{Z}_2)(\mathbf{k}_2.\mathbf{Z}_1), \tag{3.17}$$

and it can be verified that (3.14) then satisfies (3.13) correct to second order in wave amplitude. Higher-order coefficients will not be needed.

We substitute the expansion (3.14) into the Lagrangian (3.12). After spatial (but not temporal) averaging we obtain the Lagrangian for the wave amplitudes

$$L = L_2 + L_{\text{int}}, \tag{3.18}$$

with a quadratic part

$$L_2 = \tfrac{1}{2}\sum_0 \frac{\gamma_0}{\omega_0^2}\left\{i\omega_0(\dot{a}_0 a_{\bar{0}} - a_0\dot{a}_{\bar{0}}) + \left(1+\frac{f^2}{\omega_0^2}\frac{\beta_0^2}{k_0^2}\right)\dot{a}_0\dot{a}_{\bar{0}}\right\} \tag{3.19}$$

and an interaction part of the form

$$L_{\text{int}} = \sum_{0,1,2}\{a_0a_1a_2A_{012} + \dot{a}_0a_1a_2B_{012} + \dot{a}_0\dot{a}_1a_2C_{012}\}\exp\{-i(\omega_0+\omega_1+\omega_2)t\} + \ldots, \tag{3.20}$$

in which A_{012}, etc., differ from zero only when $\mathbf{k}_0+\mathbf{k}_1+\mathbf{k}_2 = 0$, since no other cubic terms survive the spatial averaging. We are here assuming spatial *homogeneity*, i.e. that the wave amplitudes a_j are functions of time alone, to sufficient accuracy.

We assume now that because of nonlinear interaction the amplitudes of the linear wave field show only a slow variation in time compared with the rapid variation of the phase. Then, applying the usual two-timing analysis, the equation of motion for the wave amplitude

$$\frac{d}{dt}\frac{\partial L}{\partial \dot{a}_{\bar{0}}} - \frac{\partial L}{\partial a_{\bar{0}}} = 0 \tag{3.21}$$

is given to the lowest order in $\dot{a}/\omega a \ll 1$ by

$$\dot{a}_0 = -3i\omega_0\gamma_0^{-1}\sum_{12} a_1a_2D_{\bar{0}12}\exp i(\omega_0-\omega_1-\omega_2)t, \tag{3.22}$$

with an interaction coefficient

$$D_{\bar{0}12} = -\tfrac{1}{2}A_{\bar{0}12} + \tfrac{1}{6}i(\omega_0-\omega_1-\omega_2)B_{\bar{0}12}. \tag{3.23}$$

Equation (3.22) may be solved by a perturbation analysis for either small amplitudes ($a \ll 1$) or small coupling ($D \ll 1$). It is found then that pairs of waves generate oscillations with the sum and the difference of their wave vectors and frequencies. The oscillations remain stationary unless the resonance condition

$$\omega_0-\omega_1-\omega_2 = 0 \tag{3.24}$$

is met. Then energy is transferred from the generating components $(s_1, \mathbf{k}_1)$ and $(s_2, \mathbf{k}_2)$ to a free wave $(s_0, \mathbf{k}_0)$.

On the resonance surface $\omega_0+\omega_1+\omega_2=0$ the interaction coefficient takes the symmetrical form

$$D_{012} = -\tfrac{1}{2}A_{012} = \alpha_{012}+\alpha_{102}+\alpha_{210}, \tag{3.25}$$

with

$$\alpha_{012} = \tfrac{1}{12}iC_0(\omega_0^2-f^2)\,(\mathbf{k}_1.\mathbf{Z}_2)\,(\mathbf{k}_2.\mathbf{Z}_1). \tag{3.26}$$

The symmetrization of A_{012} in the three index pairs follows from the structure of the interaction Lagrangian (3.20). Because of reality we have

$$A_{\bar{0}\bar{1}\bar{2}} = (A_{012})^*; \tag{3.27a}$$

and, as already mentioned, homogeneity implies

$$A_{012} = 0 \quad \text{for} \quad \mathbf{k}_0+\mathbf{k}_1+\mathbf{k}_2 \neq 0. \tag{3.27b}$$

Furthermore, one finds

$$A_{012} = 0 \quad \text{for} \quad \mathbf{k}_0 = 0. \tag{3.28}$$

The same relations apply of course to D_{012}.

3.3. *The radiation balance equation*

We shall consider only average properties of the internal wave field. To a first approximation, the wave field is statistically stationary and homogeneous, so that ensemble mean values may be obtained by applying time or spatial averaging procedures to the data. The statistical properties of a stationary and homogeneous field of free dispersive linear waves are completely determined by the ('power') spectrum since such a field rapidly attains a Gaussian state (Hasselmann 1967), asymptotically for any fixed spectral resolution.

In practice, the internal wave field in the ocean is locally Gaussian, stationary and homogeneous only because nonlinear and external dynamical processes weakly affect the state of the field. The spectrum is thus a locally defined quantity which varies slowly in space and time. We define the energy spectrum $E(\mathbf{k},\mathbf{r},t)$ by

$$\langle a^s_{\mathbf{k}}(a^{s'}_{\mathbf{k}'})^*\rangle = \tfrac{1}{2}\delta_{ss'}\delta(\mathbf{k}-\mathbf{k}')\,\Delta^3k\gamma^{-1}E(\mathbf{k},\mathbf{r},t). \tag{3.29}$$

Here angle brackets denote ensemble means and Δ^3k is the wavenumber increment of the sum (3.14).

Owing to interaction processes the wave action of each individual wave component no longer remains constant but changes slowly along the wave's path. Accounting for these changes by a source function S, the generalization of (3.9) to a statistical wave field is given by the radiation balance or Boltzmann equation

$$\left\{\frac{\partial}{\partial t}+\dot{r}_j\frac{\partial}{\partial r_j}+\dot{k}_j\frac{\partial}{\partial k_j}\right\}n = S[n], \tag{3.30}$$

where

$$n(\mathbf{k},\mathbf{r},t) = E(\mathbf{k},\mathbf{r},t)/\omega(\mathbf{k}) \tag{3.31}$$

is the action density spectrum and ω is the intrinsic frequency.

At the lateral or vertical boundaries the wave packets are reflected and undergo additional changes if interactions with external fields at the boundary occur. The radiation condition at a boundary with a normal vector η_j is thus of the form

$$\eta_j\{\dot{r}_j(\mathbf{k})\,n(\mathbf{k})+\dot{r}_j(\mathbf{k}')\,n(\mathbf{k}')\} = \mathscr{F}[n], \tag{3.32}$$

where $\mathscr{F}[n]$ is the net flux of action through the boundary and $\mathbf{k}$ and $\mathbf{k}'$ the incident and reflected wave vectors of the wave packet (cf. Müller & Olbers 1975).

Because of the Gaussian property of the lowest-order wave field and its statistical independence of external fields, the radiation balance equation is a closed equation for the action density spectrum: the source function is again a functional of the spectrum. The actual form of the functional can be derived for each interaction process separately; superposition yields the complete source function S. Methods and concepts for deriving the source terms of various interaction processes affecting the internal wave field have been surveyed by Müller & Olbers (1975).

The theory of resonant interactions in statistical wave fields has been worked out by Hasselmann (1966, 1967, 1968). The equation of motion (3.22) for the wave amplitude and the relations (3.27) for the interaction coefficients are almost identical to the equations (2.7)–(2.9) of Hasselmann's (1967) paper. Thus we can refer to his derivation of the source function for wave–wave interaction and give only the final result, which is

$$S_{\mathrm{ww}} = \int d^3k_1 \int d^3k_2 \{T^+ \delta(\mathbf{k}-\mathbf{k}_1-\mathbf{k}_2)\,\delta(\omega-\omega_1-\omega_2)\,[n_1 n_2 - n n_1 - n n_2] + 2T^- \delta(\mathbf{k}-\mathbf{k}_1+\mathbf{k}_2)\,\delta(\omega-\omega_1+\omega_2)\,[n_1 n_2 + n n_1 - n n_2]\}, \quad (3.33)$$

where $n_j = n(\mathbf{k}_j)$ and ω_j (here > 0) is the intrinsic frequency of the wave component $\mathbf{k}_j$. The transfer function T^μ, $\mu = \pm$, is found to be

$$T^\mu = 18\pi \frac{\omega\omega_1\omega_2}{\gamma\gamma_1\gamma_2} |D^{-\,+\,\mu}_{-\mathbf{k}\,\mathbf{k}_1\,\mu\mathbf{k}_2}|^2. \quad (3.34)$$

Because of (3.15) and (3.26), T^μ does not depend on the normalization constant of the relative amplitudes (3.15).

The transfer function T^μ and the resonance conditions

$$\omega - \omega_1 - \mu\omega_2 = 0, \quad \mathbf{k} - \mathbf{k}_1 - \mu\mathbf{k}_2 = 0 \quad (3.35)$$

have axial symmetry with respect to the vertical axis. Therefore the source function shows vertical symmetry, or any subclass of axial symmetry with the vertical axis, if the spectrum obeys any of these symmetries. This means especially that such a symmetry class of a spectrum cannot be changed by wave–wave interactions.

The source term S_{ww} very closely resembles Boltzmann's collision integral for interacting particles of momentum $\mathbf{k}$ and energy ω distributed in $\mathbf{r}$, $\mathbf{k}$ space according to a number density n. T^μ is then the differential cross-section for the scattering process; the δ-functions in the integral express the conservation of energy and momentum for each individual collision. Consequently, the total wave energy and momentum are conserved:

$$\int d^3k \begin{Bmatrix} \omega \\ \mathbf{k} \end{Bmatrix} S_{\mathrm{ww}} = 0, \quad (3.36)$$

so that resonant interactions among the waves only redistribute energy and momentum within the wave field.

4. The nonlinear energy transfer within Garrett–Munk spectra

The source function for resonant interactions in a statistical internal wave field has been computed by Kenyon (1968), who used a model spectrum with energy in the first two modes in a linearly stratified ocean. Such a model is in strong contrast to the recent picture of the deep-sea internal wave field as described by Garrett & Munk (1972*a*, 1975). According to their model the internal wave energy extends to quite high mode numbers. The time scales of the nonlinear interactions in such a wave field, and of course the detailed features, will differ from Kenyon's results, so that a re-examination of the nonlinear energy transfer appears to be necessary.

4.1. *The Garrett–Munk model spectrum*

Based on internal wave observations made at different locations and different times, the GM model is believed to represent to some degree some average properties of the internal wave field in the ocean, such as horizontal isotropy, vertical scales of about 100 m, horizontal scales of the order of some km, and a -2 slope in the frequency domain of the horizontal kinetic energy spectrum. Some other features of the model such as the form of the bandwidth and the vertical symmetry between upward- and downward-propagating waves (inherent in the modal approach) are still questionable.

The GM model spectrum is horizontally isotropic and vertically symmetric and conveniently represented as $(\alpha, \omega, \phi, \sigma)$-density, where (α, ϕ) are polar coordinates of the horizontal wavenumber $\boldsymbol{\alpha}$ and σ the sign of the vertical wavenumber. Transformation of the energy spectrum $E(\mathbf{k})$ follows from

$$\int d^3k\, E(\mathbf{k}) = \sum_{\sigma=\pm} \int_0^\infty d\alpha \int_f^N d\omega \int_0^{2\pi} d\phi\, E^\sigma(\alpha, \omega, \phi). \tag{4.1}$$

Thus
$$E^\sigma(\alpha, \omega, \phi) = J.E(\boldsymbol{\alpha}, \sigma\beta) \tag{4.2}$$

with the Jacobian

$$J = \left| \frac{\partial(k_1, k_2, k_3)}{\partial(\alpha, \omega, \phi)} \right| = \frac{\alpha^2 \omega (N^2 - f^2)}{(N^2 - \omega^2)^{\frac{1}{2}} (\omega^2 - f^2)^{\frac{1}{2}}}. \tag{4.3}$$

For the GM model we have

$$E^+(\alpha, \omega, \phi) = E^-(\alpha, \omega, \phi) = E(\alpha, \omega), \tag{4.4}$$

which is of the form

$$E(\alpha, \omega) = \frac{E}{2} \cdot \frac{1}{2\pi_{\blacksquare}} \cdot \frac{1}{\alpha_*(\omega)} A\left(\frac{\alpha}{\alpha_*(\omega)}\right) B(\omega). \tag{4.5}$$

Here $E(r_3)$ is the total energy per unit volume of the wave field and $\alpha_*(\omega)$ the bandwidth for the horizontal wavenumber. The representation of the spectrum involves two distribution functions $A(\lambda)$ and $B(\omega)$ describing the distribution of energy in α, ω space. Both are normalized to unity. For $A(\lambda)$, GM took a simple top-hat distribution

$$A(\lambda) = \begin{cases} 1 & \text{for} \quad 0 \leqslant \lambda \leqslant 1, \\ 0 & \text{otherwise} \end{cases} \tag{4.6}$$

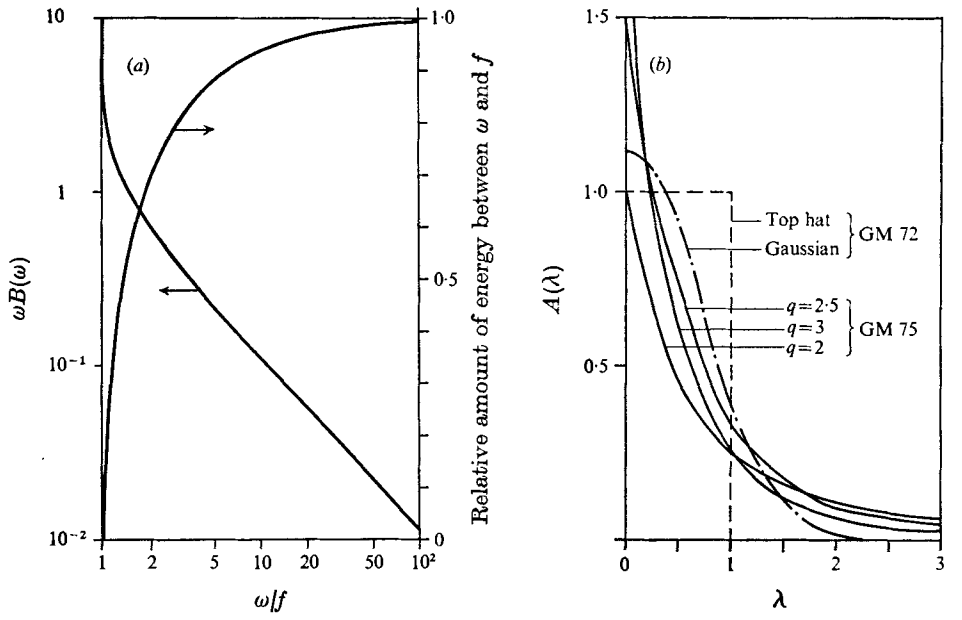

FIGURE 1. (*a*) Energy distribution function $B(\omega)$ of the GM model, and its integral from f to ω. (*b*) Energy distribution function $A(\lambda)$ of the GM model.

in their 1972 model, and

$$A(\lambda) = (q-1)(1+\lambda)^{-q} \tag{4.7}$$

in their more sophisticated 1975 model, which adjusts the model spectrum at high vertical wavenumbers to observed fine-structure spectra. The data suggest $2 < q < 3$. For the frequency distribution GM chose

$$B(\omega) = \frac{2}{\pi}\frac{f}{\omega}(\omega^2 - f^2)^{-\frac{1}{2}}, \tag{4.8}$$

which is the well-established ω^{-2} law away from f, modified by an integrable cusp at f to represent the average inertial peak. Figure 1 (*a*) shows $\omega B(\omega)$ and figure 1 (*b*) shows $A(\lambda)$ for the two models and a Gaussian curve which we shall use instead of (4.6) for numerical reasons.

For the bandwidth GM took

$$\alpha_*(\omega) = b\,.\,j_*(\omega^2 - f^2)^{\frac{1}{2}} \tag{4.9}$$

with a scaling factor $b = 4{\cdot}6 \times 10^{-3}\,\mathrm{s\,cm^{-1}}$ and an equivalent mode-number scale j_* which is 20 for GM 72 and 6 for GM 75. Recent estimates of j_* for GM 72 range from 8 to 15 (Siedler 1974; Desaubies 1975; Cairns 1975).

The energy density was found to be proportional to the buoyancy or Brunt–Väisälä frequency:

$$E(r_3) = E_0 N(r_3)/N_0, \tag{4.10}$$

which is in accordance with a linear WKBJ model [(3.8) with $\partial/\partial t = 0$] and with observations. According to Garrett & Munk (1972*a*) a representative value of the energy level is $E_0 = 30\,\mathrm{cm^2\,s^{-2}}$ at $N_0 = 5{\cdot}2 \times 10^{-3}\,\mathrm{s^{-1}}$

Besides the inertial frequency f the GM model involves three independent parameters: the wavenumber slope q, the mode-number scale j_* and the energy-level parameter E_0/N_0. For the computation of the source function we shall take $q = 2{\cdot}5$ and study only the effect of j_* and E_0/N_0 or, equivalently, the maximal bandwidth

$$k_*(r_3) = \alpha_*(N) = b\,.j_*[N^2(r_3) - f^2]^{\frac{1}{2}} \tag{4.11}$$

and the total energy density $E(r_3)$.

4.2. *Computation of the transfer integral*

As axial and vertical symmetries of the spectrum are transmitted to the source function it is convenient to rewrite the transfer integral (3.33) in a form in which the source function and the spectrum appear as $(\alpha, \omega, \phi, \sigma)$-densities. We transform the densities and the volume elements of the integration and eliminate the δ-functions. This yields

$$S^{\sigma}_{\mathrm{ww}}(\alpha,\omega,\phi) = \sum_{\sigma_1=\pm} \sum_{\mathrm{sign}\,(\phi-\phi_1)} \left\{ \int_f^{\omega-f} d\omega_1 \int_{\alpha_{1\,\min}}^{\alpha_{1\,\max}} d\alpha_1 \hat{T}^{+}[J\hat{n}_1\hat{n}_2 - J_2\hat{n}\hat{n}_1 - J_1\hat{n}\hat{n}_2] \right.$$
$$\left. + \int_{\omega+f}^{N} d\omega_1 \int_{\alpha_{1\mathrm{min}}}^{\alpha_{1\,\max}} d\alpha_1 \hat{T}^{-}[J\hat{n}_1\hat{n}_2 + J_2\hat{n}\hat{n}_1 - J_1\hat{n}\hat{n}_2] \right\}, \tag{4.12}$$

with $\hat{n} = E^{\sigma}/\omega$ and

$$\hat{T}^{\mu} = T^{\mu}(J_2\,|d\omega_2/d\phi_1|)^{-1}. \tag{4.13}$$

The quantities with subscript 2 can be eliminated using the resonance conditions (3.35) and the dispersion relation (3.5). These equations in addition determine the wavenumber interval $(\alpha_{1\,\min}, \alpha_{1\,\max})$ to which α_1 is restricted and give $|\phi - \phi_1|$ as a function of α, ω, ϕ, σ, α_1, ω_1 and σ_1.

Note that the difference interaction ($\mu = -$) contributes to S_{ww} only for $\omega < N - f$ while sum interaction ($\mu = +$) contributes only for $\omega > 2f$. Obviously $S_{\mathrm{ww}} \equiv 0$ for $N \leqslant 2f$: the resonance conditions cannot be met and triad interactions are impossible.

The form (4.12) of the transfer integral is suitable for numerical computation. The accuracy of the numerical integration, however, can be improved by two minor modifications.

(i) The transfer function $\hat{T}^{\mu}$, as defined by (4.13), has integrable singularities at $\alpha_1 = \alpha_{1\,\min}$ and $\alpha_1 = \alpha_{1\,\max}$ which originate from $|d\omega_2/d\phi_1|^{-1}$. These singularities can be separated and integrated analytically prior to the numerical integration.

(ii) Because of the symmetrical structure of the interaction coefficients (3.25) and the resulting symmetry of the transfer integral (3.33) it is possible to get three independent estimates of the source function even though the terms of the integrand are only computed once. One estimate is obtained as the direct result of the integration and two more by collecting for each resonance point $\mathbf{k}$, $\mathbf{k}_1$ and $\mathbf{k}_2$ all increments occurring at $\mathbf{k}_1$ and $\mathbf{k}_2$. It turns out that the mean of these three estimates is considerably more stable numerically than the individual estimates.

The transfer integral was evaluated for the GM spectrum. Because of the symmetry properties of this spectrum the source function $S^{\sigma}_{\mathrm{ww}}(\alpha, \omega, \phi)$ does not depend on ϕ and σ. Numerical results have been obtained using a variable-grid integration scheme to handle large variations of the integrand. The stability was tested by varying the number and the appropriate volume of the grid points. The

deviation of the three estimates from their mean as well as the conservation of energy (3.36) was used as a measure of numerical accuracy. Conservation of momentum cannot be used because it is trivially satisfied for horizontally isotropic and vertically symmetrical spectra.

The source function is parameterized by the two frequencies f and $N(r_3)$ and the parameters describing the energy spectrum, $E(r_3)$ and $k_*(r_3)$. Three of these parameters (N, E, and k_*) determine only the scale of S_{ww}. The shape of S_{ww} depends only on N/f. Thus we computed S_{ww} for different values of N/f in the range 10–100 to determine the depth dependence. For $f = 7 \times 10^{-5}\,\mathrm{s}^{-1}$ (at a latitude of 30°) this covers N from $7 \times 10^{-4}\,\mathrm{s}^{-1}$ to $7 \times 10^{-3}\,\mathrm{s}^{-1}$. As a typical main thermocline value we shall take $N = 2{\cdot}5 \times 10^{-3}\,\mathrm{s}^{-1}$, i.e. $N/f = 37{\cdot}5$. The parameters E and k_* then follow from (4.10) and (4.11) (cf. table 1).

4.3. *Characteristic features of the energy transfer*

We shall discuss the energy source function ωS_{ww} rather than the action source function S_{ww}. The graphical display is most conveniently done on a (α, β)-contour chart since here the cuts along constant α, β or ω are simply straight lines.

In order to separate scale from shape effects we introduce dimensionless shape functions of the GM model spectrum by

$$\sum_{\sigma} \int d\phi\, E^{\sigma}(\alpha, \beta, \phi) = \frac{E}{k_*^2}\, G(\alpha', \beta'; N/f), \tag{4.14}$$

and the corresponding energy source function by

$$\sum_{\sigma} \int d\phi \omega S^{\sigma}(\alpha, \beta, \phi) = \frac{E^2}{N}\, H(\alpha', \beta'; N/f), \tag{4.15}$$

where $$\alpha' = \alpha/k_* \quad \text{and} \quad \beta' = \beta/k_*$$

are scaled wavenumbers. Figures 2(*a*) and 2(*b*) are contour charts of the shape functions G and H for the GM 72 model with the Gaussian cut-off. Note that k_* is the effective bandwidth in the β direction, whence the effective α bandwidth is about $k_* \times f/N$.

Pronounced features of the energy transfer occur in the region $\beta/k_* < 3$, $N\alpha/f k_* < 3$ and $\omega < 10f$. For higher wavenumbers and frequencies the source function decreases rapidly to zero. The reason is the high energy concentration at low frequencies. Only about 10 % of the total energy is found at frequencies $\omega > 5f$ and wavenumbers $\beta > 1{\cdot}5k_*$ or $\alpha > 1{\cdot}5k_* f/N$. Restricted by the resonance conditions, the transfer can be important only at values of α, β and ω smaller than twice these limiting values.

There is removal of energy from the frequency band $2f < \omega < 5f$ at intermediate wavenumbers. The energy is transferred to high wavenumbers at low and high frequencies in a ratio of about 5:1. This result is also apparent in the one-dimensional source functions, which are projections of ωS_{ww} onto one-dimensional curves in $\mathbf{k}$ space. The shape function of the projection onto the vertical wavenumber is

$$H_1(\beta'; N/f) = \int_0^{\infty} d\alpha'\, H(\alpha', \beta'; N/f) \tag{4.16}$$

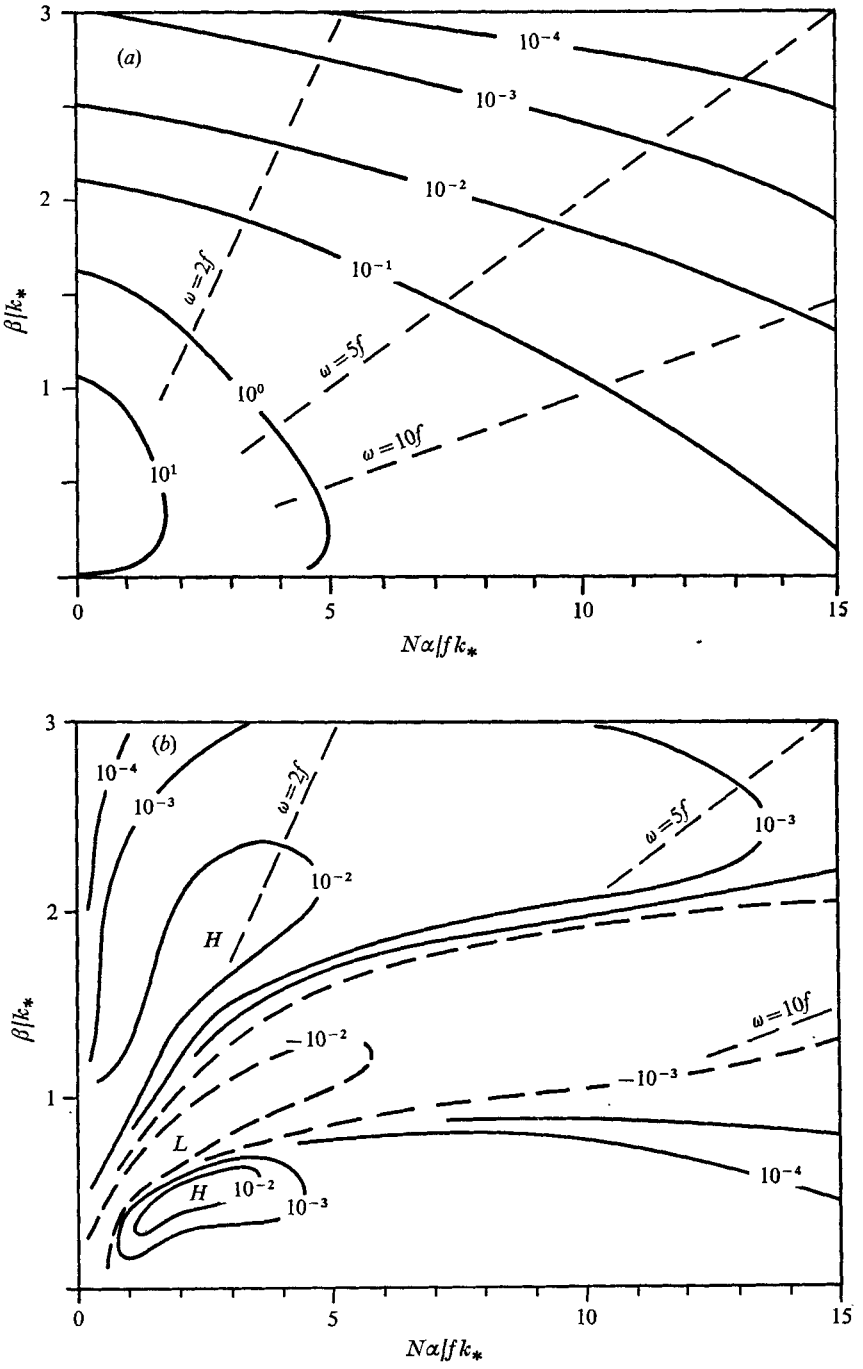

FIGURE 2. Contour chart of (*a*) the dimensionless energy spectrum $G(\alpha', \beta'; N/f)$ and (*b*) the dimensionless energy source function $H(\alpha', \beta'; N/f)$ for GM 72; $N/f = 37{\cdot}5$.

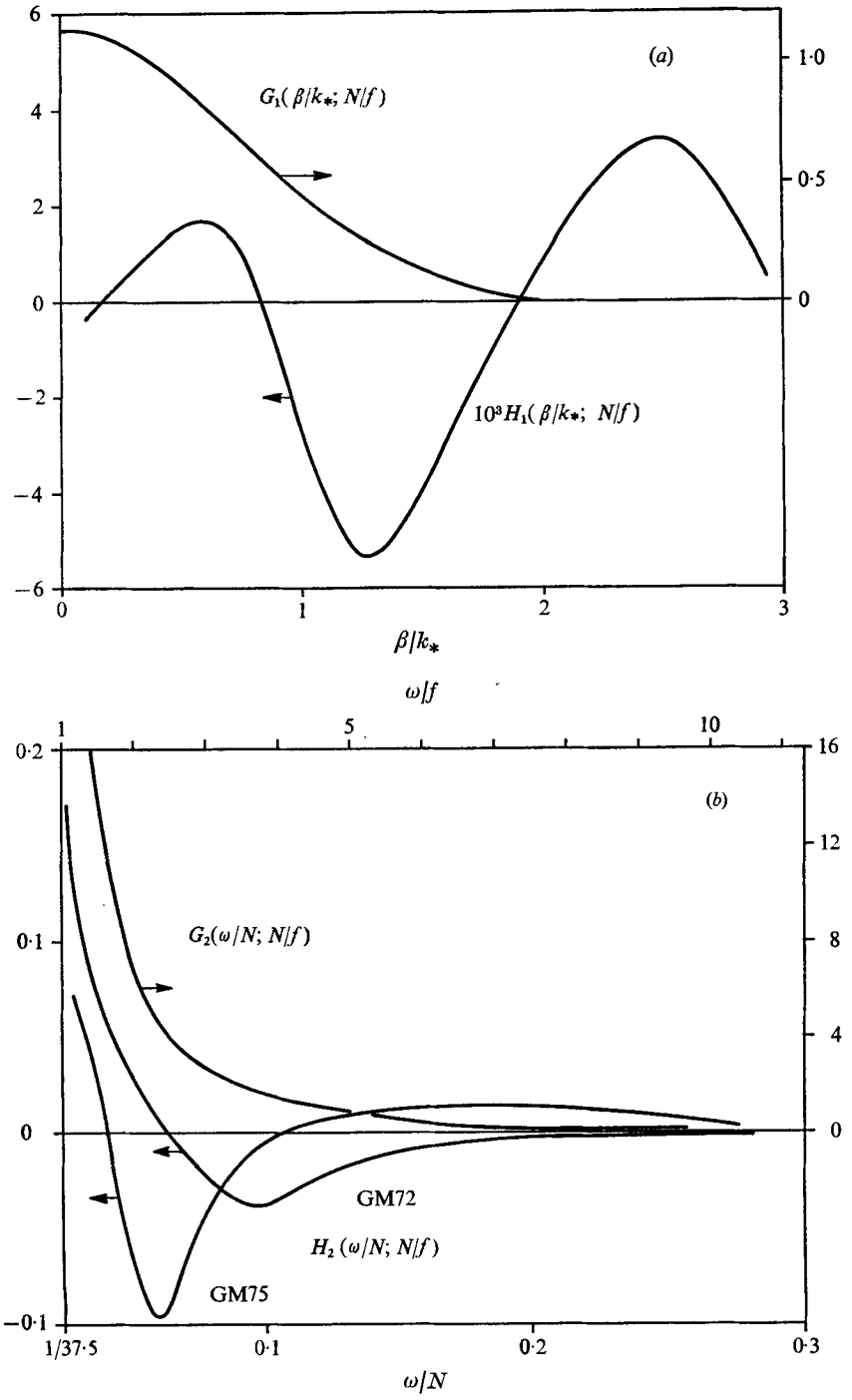

FIGURE 3. (*a*) Dimensionless projections $G_1(\beta'; N/f)$ of the energy spectrum and $H_1(\beta'; N/f)$ of the energy source function for GM 72; $N/f = 37{\cdot}5$. (*b*) Dimensionless projections $G_2(\omega'; N/f)$ of the energy spectrum for GM 72 and $H_2(\omega'; N/f)$ of the energy source function for GM 72 and GM 75; $N/f = 37{\cdot}5$.

and onto the frequency is

$$H_2(\omega'; N/f) = \int_0^\infty d\alpha' \, H\left(\alpha', \alpha'\left(\frac{1-\omega'^2}{\omega'^2 - f'^2}\right)^{\frac{1}{2}}; N/f\right), \tag{4.17}$$

where

$$\omega' = \omega/N \tag{4.18}$$

is the scaled frequency. Figures 3(*a*) and (*b*) show these shape functions together with the corresponding projections $G_1(\beta'; N/f)$ and $G_2(\omega'; N/f)$ of the spectral shape function $G(\alpha', \beta'; N/f)$.

The two-dimensional shape functions G and H for GM 75 are shown in figures 4(*a*) and (*b*). The transfer within this spectrum is similar to that within the GM 72 spectrum. The lobes extend to slightly higher wavenumbers because the energy distribution of GM 75 decreases more slowly in wavenumber space than GM 72 (cf. figure 1*b*). A minor difference occurs in the ratio of the transfer rates to low and high frequencies, which are nearly equal for GM 75. The projection of the shape function onto frequency (figure 3*b*) and the projection onto vertical wavenumber (figure 5) are similar to those of GM 72 with the exception of $H_1(\beta'; N/f)$ at low vertical wavenumbers: the positive transfer to low vertical wavenumbers at high frequencies is completely masked by the energy loss at lower frequencies.

The transition from the scaled shape functions to real transfer rates follows from (4.14) and (4.15). Table 1 gives the scaling factors and values for the main thermocline. To get an impression of the importance of the energy transfer in the different spectral regions note that Ht/τ_* represents the amount the scaled spectrum G would change if the transfer rate remained constant at its initial value over a time t (this applies to the projections as well). Here $\tau_* = N/k_*^2 E$ is about 3×10^3 s for GM 72 and $3{\cdot}6 \times 10^4$ s for GM 75 in the main thermocline. Thus, for example, $10^2 H$ for GM 72, or $10H$ for GM 75, is the amount G would change in 3 days.

The strength of the interaction may be characterized by integral transfer rates

$$\Delta\dot{E} = N^{-1} E^2 k_*^2 \int d\alpha' \, d\beta' \, H(\alpha', \beta'; N/f) \tag{4.19}$$

and characteristic transfer times

$$\tau = |E/\Delta\dot{E}| = N k_*^{-2} E^{-1} \left| \int d\alpha' \, d\beta' \, H(\alpha', \beta'; N/f) \right|^{-1}, \tag{4.20}$$

integrating over different spectral regions. In the main thermocline we get typically

$$\Delta\dot{E} = 10^{-5} \, \mathrm{cm^2 \, s^{-3}} \tag{4.21}$$

and

$$\tau = 10 \text{ days}. \tag{4.22}$$

GM 72 generally yields slightly larger transfer rates than GM 75.

As they are based on the GM model, the values apply to average conditions in the ocean. Nevertheless, we should regard them as estimates which may vary by an order of magnitude because of local variations of the spectrum. The transfer rate $\Delta\dot{E}$ increases quadratically with the local energy density E and the local

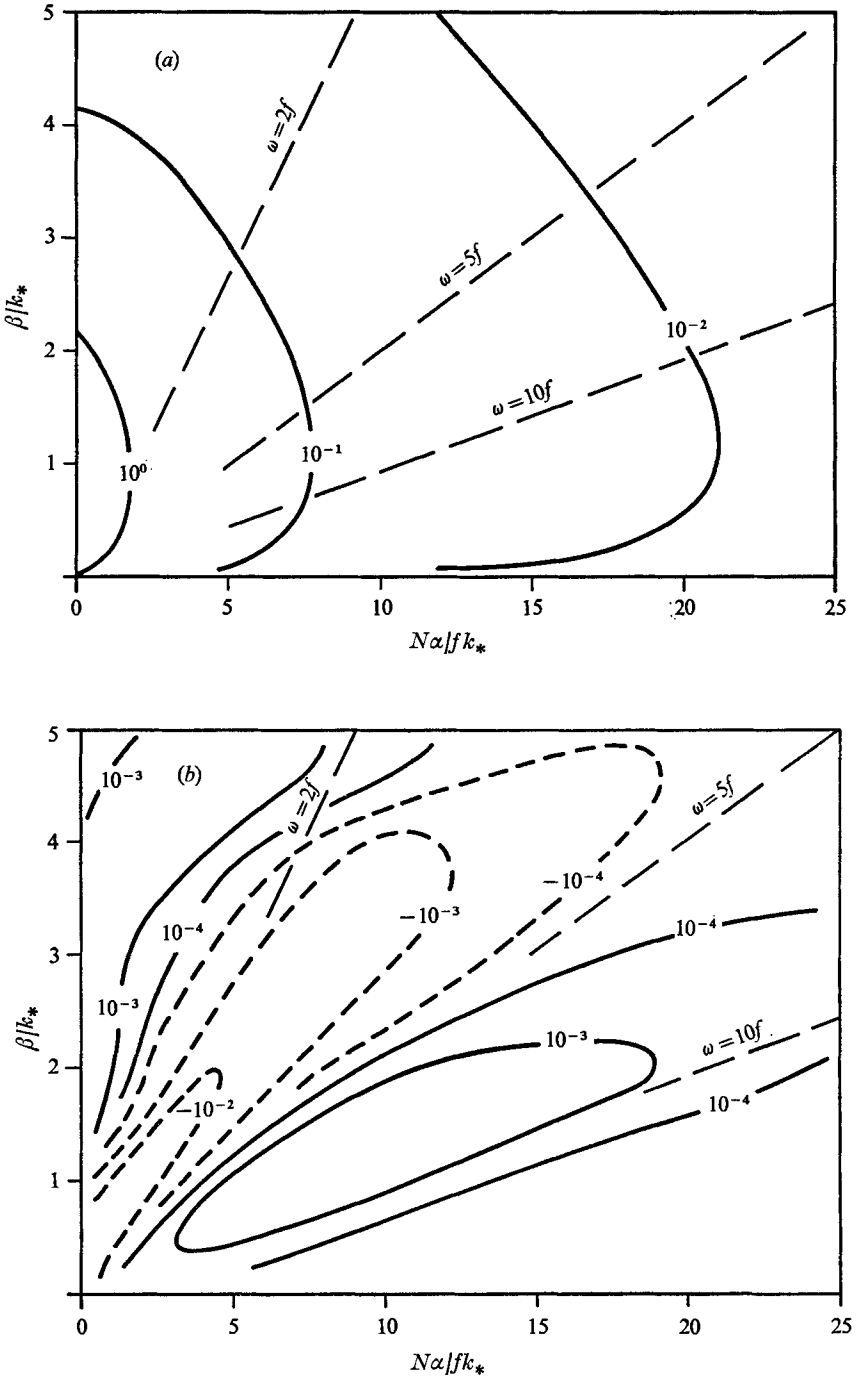

FIGURE 4. Contour chart of (*a*) the dimensionless energy spectrum $G(\alpha', \beta'; N/f)$ and (*b*) the dimensionless energy source function $H(\alpha', \beta'; N/f)$ for GM 75; $N/f = 37{\cdot}5$.

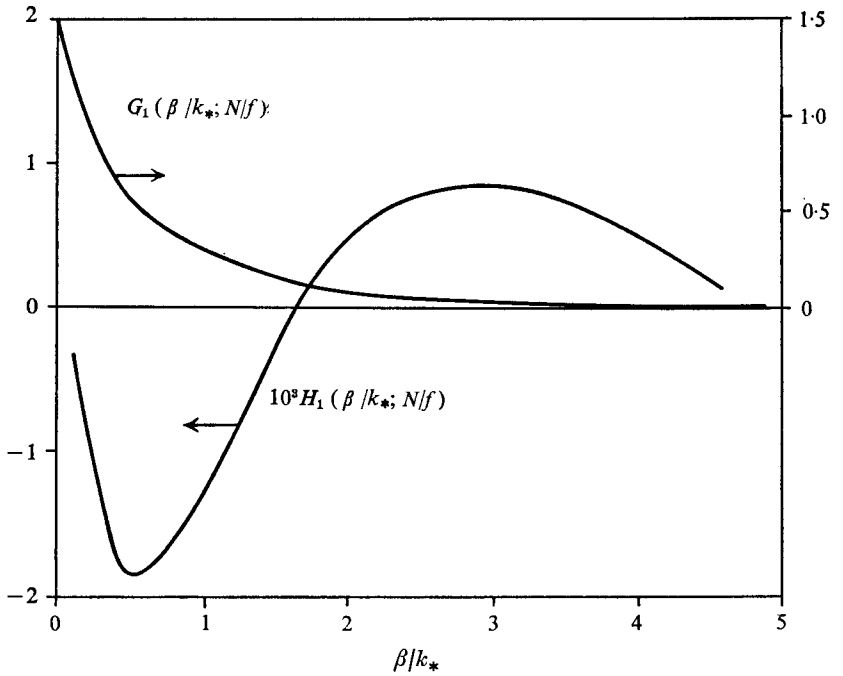

FIGURE 5. Dimensionless projection $G_1(\beta'; N/f)$ of the energy spectrum and dimensionless projection $H_1(\beta'; N/f)$ of the energy source function for GM 75; $N/f = 37{\cdot}5$.

	Scaling factor	Main thermocline value	
		GM 72	GM 75
Brunt–Väisälä frequency	N	$2{\cdot}5 \times 10^{-3}$	
Energy level	E	15·0	
Bandwidth	k_*	$2{\cdot}3 \times 10^{-4}$	$0{\cdot}7 \times 10^{-4}$
Spectrum $G(\alpha', \beta'; N/f)$	E/k_*^2	$2{\cdot}8 \times 10^{8}$	$3{\cdot}1 \times 10^{9}$
$G_1(\beta'; N/f)$	E/k_*	$6{\cdot}2 \times 10^{4}$	$2{\cdot}1 \times 10^{5}$
$G_2(\omega'; N/f)$	E/N	6×10^{3}	6×10^{3}
Source function $H(\alpha', \beta'; N/f)$	E^2/N	9×10^{4}	9×10^{4}
$H_1(\beta'; N/f)$	E^2k_*/N	$2{\cdot}2 \times 10^{1}$	6.3
$H_2(\omega'; N/f)$	$E^2k_*^2/N^2$	2·1	$1{\cdot}8 \times 10^{-1}$
Transfer rate, $\Delta\dot{E}$	$E^2k_*^2/N$	$5{\cdot}1 \times 10^{-3}$	$4{\cdot}4 \times 10^{-4}$
Time scale, τ	$N/(k_*^2E)$	$2{\cdot}9 \times 10^{3}$	$3{\cdot}4 \times 10^{4}$

TABLE 1. Scaling factors, all values in cgs units.

bandwidth k_*. Local variations in E by a factor of 2 to 3 are frequently observed; similar variations can be expected for k_*.

The shape function $H(\alpha', \beta'; N/f)$ has been computed for different ratios N/f to obtain the depth dependence of the source function and related quantities. In the interval $10 < N/f < 100$ the structure of H does not change significantly.

The level of H varies approximately as $(N/f)^{-1}$. Hence the integral transfer rate (4.19) behaves with depth according to

$$\Delta\dot{E} \sim (Ek_*/N)^2 \sim N^2, \tag{4.23}$$

so that characteristic transfer time is proportional to the Brunt–Väisälä period:

$$\tau \sim N^2/Ek_*^2 \sim N^{-1}. \tag{4.24}$$

Both relations indicate that nonlinear wave–wave interactions are most rapid in the main thermocline. Using (4.23) the transfer rate per unit surface area can be determined. For an exponential N-profile with an e-folding length of 1·3 km (cf. Garrett & Munk 1972) we get

$$\Delta\dot{\mathcal{E}} = \int_{-\infty}^{0} dr_3 \Delta\dot{E} = 3\,\mathrm{cm^3\,s^{-3}}. \tag{4.25}$$

5. Implications for the energy balance

Besides nonlinear interactions among the waves there are other processes which affect the state of the wave field. Internal waves can be excited and dissipated by various mechanisms (see the review by Thorpe 1975); even other energy-conserving transfer processes are possible. A survey of these processes, their theoretical treatment, and the form of the corresponding source terms in the radiation balance equation has recently been given by Müller & Olbers (1975). They point out that the efficiency of many interaction processes at generating, dissipating or transferring internal wave energy can hardly be estimated, partly because external fields involved in the interaction are not sufficiently well known (this applies for instance to atmospheric forcing), partly because the evaluation of the source term describing the interaction is cumbersome and needs numerical analysis (just as in most resonant interaction problems), and partly because reasonable models of the interaction process are missing (e.g. for strongly nonlinear processes).

A few processes have been studied for oceanic conditions within a framework which is applicable to the energy balance of the deep-sea internal wave field. These are the WKBJ interaction of a quasi-geostrophic mean flow with the internal wave field (Müller 1974), the generation of lee waves by steady and tidal currents (Bell 1975), the scattering of internal waves by the fine-structure of the stratification (Mysak & Howe 1975), and the present study of wave–wave interactions within the internal wave field.

Though we do not know the effect of each individual process affecting the wave field we know what they all do in concert on the average in the ocean: their sum maintains the internal wave climate represented by the universally observed frequency spectrum or, as a first attempt at reconstructing the complete spectrum, the GM model. Thus, with the effect of the wave–wave interactions as a backbone, we may look for the implications for other interaction processes which take part in the energy balance.

In order to explain a climatic state of the wave field we have to look for interaction processes which are able to balance the sources and sinks in the spectrum

originating from the wave–wave interactions. Referring to figures 2 and 4, we expect an input of energy at low vertical and horizontal wavenumbers in the frequency band $2f < \omega < 5f$, and dissipation of energy at high vertical wavenumbers and $\omega \lesssim 2f$, and at high horizontal wavenumbers and $\omega \gtrsim 5f$. It is unlikely that this will be achieved by one process alone. A possible energy balance which approximately satisfies the above restrictions has been discussed by Müller & Olbers (1975): the wave field is driven at low wavenumbers by a larger-scale mean flow, and the energy is dissipated after transfer to high wavenumbers by wave–wave interactions and subsequent wave breaking.

5.1. *Inertial waves*

Let us first consider the near-inertial frequency band. Both spectral models, GM 72 and GM 75, very efficiently produce near-inertial waves of high wavenumber. The small inertial peak of the models represented by the cusp in (4.7) at $\omega = f$ is not responsible for this feature. The energy is mainly taken from the continuum. This was tested by evaluating the source function for a frequency distribution function $B(\omega) = f/\omega^2$, for which the transfer to near-inertial waves is even slightly higher than for (4.7).

The growth of the spectrum which is caused by the nonlinear transfer must of course be limited by a dissipation mechanism. The balance may be written in the simplified form

$$\dot{E}_{\mathrm{I}} = -E_{\mathrm{I}}/\tau_{\mathrm{ds}} + E_{\mathrm{C}}/\tau, \tag{5.1}$$

where E_{I} is the energy in the high wavenumber inertial band, and τ_{ds} a characteristic dissipation time. The nonlinear transfer to the inertial band is the integral of ωS_{ww} over this spectral region. As the energy comes from the continuum, we have approximated the transfer by E_{C}/τ, where E_{C} is the energy in the continuum and τ the characteristic transfer time (4.20).

In a steady state the energy level in the inertial band is determined via

$$E_{\mathrm{I}} = (\tau_{\mathrm{ds}}/\tau)\, E_{\mathrm{C}} \tag{5.2}$$

through the dissipation time τ_{ds} and the nonlinear transfer. An energy level E_{I} much smaller than E_{C}, as claimed by the GM model, would then imply $\tau_{\mathrm{ds}} \ll \tau$, i.e. very effective dissipation.

Similar arguments may be applied to inertial waves in the main region of the spectrum (i.e. $\beta < k_*$). The tongue of the nonlinear transfer extends to this region at least for GM 72 (see figure 2*b*). In this case we need no direct generation process of inertial waves by external fields, e.g. the atmosphere, but instead we need a dissipation mechanism which destroys the energy input from the internal wave continuum due to wave–wave interactions. Since the energy in the inertial peak is comparable to or even larger than E_{C} the relation (5.2) implies $\tau_{\mathrm{ds}} \gtrsim \tau$.

Generation of inertial waves out of the continuum by wave–wave interactions would explain the lack of coherence between deep-sea inertial waves and atmospheric fields (e.g. Pollard 1970). If generated by wave–wave interactions, modulations of inertial energy should correlate with modulations at higher frequencies. Correlations of this kind have been found by Frankignoul (1974).

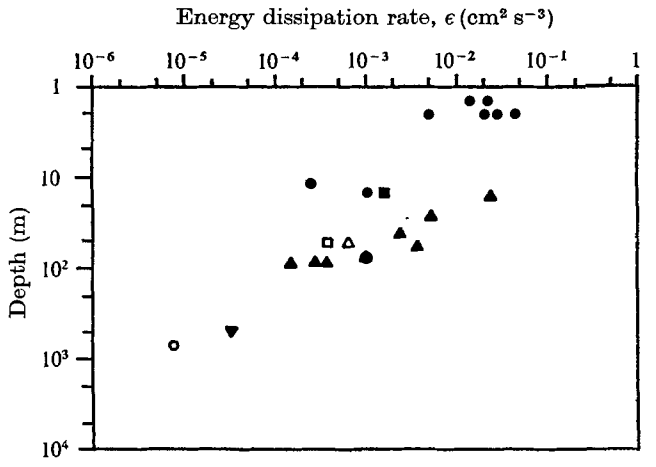

FIGURE 6. Depth variation of the energy dissipation rate (after Okubo 1970). ●, Stewart & Grant (1962); ■, Grant *et al.* (1962); ▼, Takenouti *et al.* (1962); ▲, Grant *et al.* (1968); □, Woods (1968); △, Thorpe (1973); ○, our value.

5.2. *Dissipation by wave breaking*

Dissipation at high wavenumbers may be caused by wave breaking. This assumption has been made by Bretherton (1969) to explain clear-air turbulence as the result of a nonlinear cascade in the internal wave spectrum to high wavenumbers and subsequent breaking by Kelvin–Helmholtz instability.

There is direct and indirect evidence of wave breaking in the ocean. Deep-sea observations of temperature inversions and their evolution time have been reported by Cairns (1975). Pictures of the flow pattern in the Mediterranean summer thermocline showing internal wave breakers have been presented by Woods (1968). He found (see also Woods & Wiley 1972) that breaking occurs rather intermittently and produces discrete, small patches of weak turbulence which spread horizontally, forming layers of homogeneous water with lenses of weak turbulence. This layered structure (fine-structure) has been observed in temperature and salinity profiles almost everywhere in the ocean (see the reviews of Monin 1973; Gregg 1975), giving indirect evidence of wave breaking.

There are several mechanisms by which internal waves may break (Turner 1973), some of which have been studied in laboratory experiments (e.g. McEwan 1971, 1973; Thorpe 1973) and in numerical models (e.g. Orlanski & Ross 1973). In the ocean, breaking by Kelvin–Helmholtz instability seems to be more likely than overturning (Garrett & Munk 1972*b*).

Independently of the detailed mechanism of the breaking process, part of the dissipated wave energy will be fed into small-scale turbulence which will be finally dissipated by molecular processes, and part of it will be used for mixing, thus eroding the mean density gradient. This balance may be written as

$$\Delta \dot{E}_{\mathrm{hw}} = \epsilon + \kappa_{\mathrm{v}} N^2, \tag{5.3}$$

where $\Delta \dot{E}_{\mathrm{hw}}$ is the nonlinear transfer to high wavenumbers, ϵ is the viscous dissipation rate and κ_{v} is the vertical eddy diffusivity. The dissipation rate ϵ and

the gain of mean potential energy $\kappa_v N^2$ are presumably of the same order of magnitude. Thorpe (1973) suggests from tank experiments a ratio $\epsilon/(\kappa_v N^2) \approx 3$, so that with $\Delta\dot{E}_{hw} = 10^{-5}\,\mathrm{cm^2\,s^{-3}}$ in the main thermocline we get

$$\left.\begin{aligned}\kappa_v &= 0{\cdot}3\,\mathrm{cm^2\,s^{-1}},\\ \epsilon &= 7{\cdot}5\times10^{-6}\,\mathrm{cm^2\,s^{-3}}.\end{aligned}\right\} \tag{5.4}$$

Neither quantity has been measured directly. Estimates depend strongly on the depth and the scale of the turbulent elements. Estimates for κ_v range from $1{\cdot}3\,\mathrm{cm^2\,s^{-1}}$ (Munk 1966) to $0{\cdot}2\,\mathrm{cm^2\,s^{-1}}$ (Roether, Muennich & Östlund 1970; Rooth & Östlund 1972), the latter figure being obtained by fitting profiles of temperature and radioactive tracers to a balance of upwelling, diffusion and decay. An estimate of $0{\cdot}3\,\mathrm{cm^2\,s^{-1}}$ for small-scale vertical diffusion has been determined by Woods & Wiley (1972) from multisheet ensembles. Estimates of the dissipation rate ϵ have been collected by Okubo (1970) for the upper 100 m of the ocean. By extrapolation to greater depths Okubo expects an abyssal ϵ of order 10^{-6} to $10^{-5}\,\mathrm{cm^2\,s^{-3}}$. This would be in good agreement with the balance (5.3) (see figure 6). Even the depth dependence of $\Delta\dot{E}_{hw} \sim N^2$ is consistent with the rather narrow range of the estimates of κ_v and a decrease of ϵ with depth.

6. Conclusion

Wave–wave interactions redistribute the energy of the wave field in wavenumber–frequency space. We have shown that the interactions within the GM-model spectra lead to a transfer of energy from low wavenumbers and intermediate frequencies to high wavenumbers and low and high frequencies. The dependence of the transfer rate on the energy level and the wavenumber bandwidth was obtained by scaling; the dependence on the depth was studied numerically. It was found that the process is most important at high values of the Brunt–Väisälä frequency, and in particular that the characteristic time scale of the nonlinear transfer varies as the Brunt–Väisälä period. For typical conditions in the ocean the time scale is of the order of some days, indicating that wave–wave interactions play an important role in the energy balance of the internal wave spectrum.

Wave–wave interactions conserve the energy and momentum of the wave field and therefore drop out of the overall energy budget, which is determined by generation and dissipation processes alone. However, if the nonlinear transfer is strong enough it may be crucial for the detailed energy balance, e.g. when generation and dissipation occur at different scales. Then the detailed form of the nonlinear transfer implies restrictions on the strength of generation and dissipation processes in the different wavenumber and frequency bands. This concept seems to be appropriate if the effect of processes cannot be estimated directly, which is the case for most generation processes because the space–time structure of the generating fields is only insufficiently known. Moreover, the energy balance is perhaps the only way to gain some insight into the effectiveness of strongly nonlinear processes.

Assuming that the nonlinear transfer to high wavenumbers is balanced by wave breaking and then partly used for mixing, we have estimated the dissipation rate of small-scale turbulence and a vertical mass diffusivity. The estimates agree well with earlier values obtained by different methods. As the nonlinear transfer feeds very efficiently the inertial band out of the internal wave continuum we suggest that the deep-sea inertial peak is to some extent generated by wave–wave interactions. The inertial energy level would then be determined by the nonlinear transfer rate and a dissipation time scale.

Features of nonlinear interactions in the wave field and ideas about the energy balance can be principally tested against observations by bispectral analysis or study of the time variability of the interacting fields. Bispectra have been reported by Neshyba & Sobey (1975) and are computed for the IWEX data (M. G. Briscoe, personal communication). Comparing the duration of IWEX with the characteristic time scales of the interaction processes, the investigation of time variability with these data seems to be marginally fruitful.

This research was supported by the Deutsche Forschungsgemeinschaft. Partial support under IDOE/NST grant GX29033 to Harvard University for general support of the MODE theoretical panel is achnowledged. The work reported here is a refinement of the author's Ph.D. thesis (Universität Hamburg, 1974). The advice and guidance of K. Hasselmann is gratefully acknowledged and thanks are expressed to P. Müller for numerous helpful discussions.

REFERENCES

BALL, F. K. 1964 Energy transfer between external and internal gravity waves. *J. Fluid Mech.* **19**, 465–478.

BELL, T. H. 1975 Topographically generated internal waves in the open ocean. *J. Geophys. Res.* **80**, 320–327.

BRETHERTON, F. P. 1969 Waves and turbulence in stably stratified fluids. *Radio Sci.* **4**, 1279–1287.

BRETHERTON, F. P. 1971 The general linearized theory of wave propagation. In *Mathematical Problems in the Geophysical Sciences*, vol. 1 (ed. W. H. Reid), pp. 61–102. Providence, R.I.: Am. Math. Soc.

BRETHERTON, F. P. & GARRETT, C. J. R. 1968 Wave trains in inhomogeneous moving media. *Proc. Roy. Soc.* A **302**, 529–554.

BRISCOE, M. G. 1975*a* Internal waves in the ocean. *Rev. Geophys. Space Phys.* **13**, 591–598, 636–645.

BRISCOE, M. G. 1975*b* Preliminary results from the tri-moored internal wave experiment (IWEX). *J. Geophys. Res.* **80**, 3872-3884.

CAIRNS, J. L. 1975 Internal wave measurements from a midwater float. *J. Geophys. Res.* **80**, 299–360.

DESAUBIES, Y. J. F. 1975 A linear theory of internal wave spectra and coherences near the Väisälä frequency. *J. Geophys. Res.* **80**, 895–899.

DEWAR, R. L. 1970 Interaction between hydromagnetic waves and a time-dependent, inhomogeneous medium. *Phys. Fluids*, **13**, 2710–2720.

DOUGHERTY, J. P. 1970 Lagrangian methods in plasma physics. Part 1. *J. Plasma Phys.* **4**, 761–785.

FOFONOFF, N. P. & WEBSTER, F. 1971 Current measurements in the western Atlantic. *Phil. Trans.* A **270**, 423–436.

FRANKIGNOUL, C. J. 1974 Preliminary observations of internal wave energy flux in frequency, depth-space. *Deep-Sea Res.* **21**, 895–899.

GARRETT, C. J. R. & MUNK, W. 1972*a* Space-time scales of internal waves. *Geophys. Fluid Dyn.* **2**, 225–264.

GARRETT, C. J. R. & MUNK, W. 1972*b* Oceanic mixing by breaking of internal waves. *Deep-Sea Res.* **19**, 823–832.

GARRETT, C. J. R. & MUNK, W. 1975 Space-time scales of internal waves: a progress report. *J. Geophys. Res.* **80**, 291–298.

GRANT, H. L., MOILLIET, A. & VOGEL, W. M. 1968 Some observations of the occurrence of turbulence in and above the thermocline. *J. Fluid Mech.* **34**, 443–448.

GRANT, H. L., STEWART, R. W. & MOILLIET, A. 1962 Turbulent spectra from a tidal channel. *J. Fluid Mech.* **12**, 241–268.

GREGG, M. C. 1975 Oceanic fine and microstructure. *Rev. Geophys. Space Phys.* **13**, 586–591.

HASSELMANN, K. 1966 Feynman diagrams and interaction rules of wave–wave scattering processes. *Rev. Geophys. Space Phys.* **4**, 1–32.

HASSELMANN, K. 1967 Nonlinear interactions treated by the methods of theoretical physics (with applications to the generation of waves by wind). *Proc. Roy. Soc.* A **299**, 77–100.

HASSELMANN, K. 1968 Weak interaction theory of ocean waves. *Basic Develop. Fluid Dyn.* **2**, 117–182.

HASSELMANN, K. *et al.* 1973 Measurements of wind–wave growth and swell decay during the Joint North Sea Wave Project (JONSWAP). *Deutsche Hydrog. Z. Suppl.* A(8°) no. 12.

HAYES, S. P., JOYCE, T. M. & MILLARD, R. C. 1975 Measurements of vertical fine structure in the Sargasso Sea. *J. Geophys. Res.* **80**, 314–319.

KENYON, K. 1968 Wave–wave interactions of surface and internal waves. *J. Mar. Res.* **26**, 208–231.

MCEWAN, A. D. 1971 Degeneration of resonantly-excited standing internal gravity waves. *J. Fluid Mech.* **50**, 431–448.

MCEWAN, A. D. 1973 Interactions between internal gravity waves and their traumatic effect on a continuous stratification. *Boundary-Layer Met.* **5**, 159–175.

MCEWAN, A. D., MANDER, D. W. & SMITH, R. K. 1972 Forced resonant second-order interaction between damped internal waves. *J. Fluid Mech.* **55**, 589–608.

MARTIN, S., SIMMONS, W. F. & WUNSCH, C. 1969 Resonant internal wave interactions. *Nature*, **224**, 1014–1016.

MARTIN, S., SIMMONS, W. F. & WUNSCH, C. 1972 The excitation of resonant triads by single internal waves. *J. Fluid Mech.* **53**, 17–44.

MONIN, A. S. 1973 Turbulence and microstructure in the ocean. *Usp. Fiz. Nauk.* (*Adv. in Pys. Sci.*) **109**, 333–354.

MORK, M. 1972 On oceanic responses to atmospheric forces. *Conseil International pour l'Exploration de la Mer*, **162**, 184–190.

MÜLLER, P. 1974 On the interaction between short internal waves and larger scale motion in the ocean. *Hamburg. Geophys. Einzelschriften*, **23**.

MÜLLER, P. & OLBERS, D. J. 1975 On the dynamics of internal waves in the deep ocean. *J. Geophys. Res.* **80**, 3848–3860.

MUNK, W. 1966 Abyssal recipes. *Deep-Sea Res.* **13**, 707–730.

MYSAK, L. A. & HOWE, M. S. 1975 A kinetic theory for internal waves in a randomly stratified ocean. *Geophys. Fluid Dyn.* (in press).

NESHYBA, S. & SOBEY, E. J. C. 1975 Vertical cross-coherence and cross-bispectra between internal waves measured in a multiple-layered ocean. *J. Geophys. Res.* **80**, 1152–1162.

OKUBO, A. 1970 Oceanic mixing. *Johns Hopkins University, Tech. Rep. Ref.* 70–1.

OLBERS, D. J. & RICHTER, A. 1973 Wave trains in the solar wind. I. General theory and its application to an ideal, isotropic one-fluid plasma. *Astrophys. Space Sci.* **20**, 373–389.

ORLANSKI, I. & ROSS, B. R. 1973 Numerical simulation of the generation and breaking of internal gravity waves. *J. Geophys. Res.* **78**, 8808–8826.

POLLARD, R. T. 1970 On the generation by winds of inertial waves in the ocean. *Deep-Sea Res.* **17**, 795–812.

ROETHER, W., MUENNICH, K. O. & ÖSTLUND, H. G. 1970 Tritium profile at the North Pacific (1969) Geosecs intercalibration station. *J. Geophys. Res.* **75**, 7672–7675.

ROOTH, C. G. & ÖSTLUND, H. G. 1972 Penetration of tritium into the Atlantic thermocline. *Deep-Sea Res.* **19**, 481–492.

SANFORD, T. B. 1975 Observations of the vertical structure of internal waves. *J. Geophys. Res.* **80**, 3861–3871.

SIEDLER, G. 1971 Vertical coherence of short-periodic current variations. *Deep-Sea Res.* **18**, 179–191.

SIEDLER, G. 1974 Observations of internal wave coherence in the deep ocean. *Deep-Sea Res.* **21**, 597–610.

STEWART, R. W. & GRANT, H. L. 1962 Determination of the rate of dissipation of turbulent energy near the sea surface in the presence of waves. *J. Geophys. Res.* **67**, 3177–3180.

TAKENOUTI, Y., NANNITI, T. & YASUI, M. 1962 The deep-current in the sea east of Japan. *Oceanog. Mag.* **13**, 89–101.

THORPE, S. A. 1966 On wave interactions in a stratified fluid. *J. Fluid Mech.* **24**, 737–751.

THORPE, S. A. 1973 Turbulence in stable stratified fluids: a review of laboratory experiments. *Boundary-Layer Met.* **5**, 95–119.

THORPE, S. A. 1975 The excitation, dissipation, and interaction of internal waves in the deep ocean. *J. Geophys. Res.* **80**, 328–338.

TURNER, J. S. 1973 *Buoyancy Effects in Fluids.* Cambridge University Press.

WEBSTER, F. 1972 Estimates of the coherence of ocean currents over vertical distances. *Deep-Sea Res.* **19**, 35–44.

WHITHAM, G. B. 1965 A general approach to linear and nonlinear dispersive waves using a Lagrangian. *J. Fluid Mech.* **22**, 273–283.

WHITHAM, G. B. 1970 Two-timing, variational principles and waves. *J. Fluid Mech.* **44**, 373–395.

WOODS, J. D. 1968 Wave-induced shear instability in the summer thermocline. *J. Fluid Mech.* **32**, 791–800.

WOODS, J. D. & WILEY, R. L. 1972 Billow turbulence and ocean microstructure. *Deep-Sea Res.* **19**, 87–121.

WUNSCH, C. 1975 Deep ocean internal waves: what do we really know? *J. Geophys. Res.* **80**, 339–343.